

## Video Article

# 3D Microtissues for Injectable Regenerative Therapy and High-throughput Drug Screening

Yaqian Li<sup>1,2</sup>, Xiaojun Yan<sup>\*1</sup>, Wei Liu<sup>\*1</sup>, Lyu Zhou<sup>1,3</sup>, Zhifeng You<sup>1</sup>, Yanan Du<sup>1,2</sup><sup>1</sup>Department of Biomedical Engineering, School of Medicine, Tsinghua University<sup>2</sup>Collaborative Innovation Center for Diagnosis and Treatment of Infectious Diseases<sup>3</sup>School of Life Sciences, Tsinghua University

\*These authors contributed equally

Correspondence to: Yanan Du at [duyanan@tsinghua.edu.cn](mailto:duyanan@tsinghua.edu.cn)URL: <https://www.jove.com/video/55982>DOI: [doi:10.3791/55982](https://doi.org/10.3791/55982)

Keywords: Bioengineering, Issue 128, Cell therapy, high-throughput drug screening, injectable, minimally invasive, microcryogels, microtissue

Date Published: 10/4/2017

Citation: Li, Y., Yan, X., Liu, W., Zhou, L., You, Z., Du, Y. 3D Microtissues for Injectable Regenerative Therapy and High-throughput Drug Screening. *J. Vis. Exp.* (128), e55982, doi:10.3791/55982 (2017).

## Abstract

To upgrade traditional 2D cell culture to 3D cell culture, we have integrated microfabrication with cryogelation technology to produce macroporous microscale cryogels (microcryogels), which can be loaded with a variety of cell types to form 3D microtissues. Herein, we present the protocol to fabricate versatile 3D microtissues and their applications in regenerative therapy and drug screening. Size and shape-controllable microcryogels can be fabricated on an array chip, which can be harvested off-chip as individual cell-loaded carriers for injectable regenerative therapy or be further assembled on-chip into 3D microtissue arrays for high-throughput drug screening. Due to the high elastic nature of these microscale cryogels, the 3D microtissues exhibit great injectability for minimally invasive cell therapy by protecting cells from mechanical shear force during injection. This ensures enhanced cell survival and therapeutic effect in the mouse limb ischemia model. Meanwhile, assembly of 3D microtissue arrays in a standard 384-multi-well format facilitates the use of common laboratory facilities and equipment, enabling high-throughput drug screening on this versatile 3D cell culture platform.

## Video Link

The video component of this article can be found at <https://www.jove.com/video/55982/>

## Introduction

Traditional cell culture on flattened two-dimensional (2D) surfaces, such as a culture dish or multi-well plates, can hardly elicit cell behaviors close to their native states. Accurate recapitulation of native cellular microenvironments, which comprise of various cell types, extracellular matrices and bioactive soluble factors in three-dimensional (3D) architectures<sup>1,2,3,4</sup>, is essential to construct biomimicking tissues *in vitro* for applications in tissue engineering, regenerative medicine, fundamental biology research and drug discovery<sup>5,6,7,8,9</sup>.

In lieu of 2D cell culture, 3D cell culture is widely used to advance biomimetic micro-architectural and functional features of cells cultured *in vitro*. A popular 3D cell culture method is to aggregate cells into spheroids<sup>7,8,9,10</sup>. Cellular spheroids could be injected to injured tissues with enhanced cellular retention and survival in comparison to injection of dispersed cells. However, non-uniform spheroid sizes and inevitable mechanical injury imposed on cells by fluid shear force during injection lead to poor cell therapeutic effects<sup>11,12,13</sup>. Similarly, the inherent non-uniformity during aggregation of spheroids has made their translation to 3D cell-based high-throughput drug screening challenging<sup>10</sup>.

Another method for 3D cell culture is achieved with the assistance of biomaterials, which typically encapsulates cells in aqueous hydrogels or porous scaffolds. It allows for greater flexibilities in constructing 3D architectures. For therapy, cells encapsulated in bulk scaffolds are usually delivered to animal body via surgical implantation, which is invasive and traumatic, hence restricting its wide translation to bedside. On the other hand, aqueous hydrogels enable minimally invasive therapy by injecting cells suspended in hydrogel precursor solution into animal bodies, allowing *in situ* gelation via thermo-, chemical or enzymatic crosslinking<sup>11</sup>. However, as cells are delivered whilst the hydrogel precursors are still in an aqueous state, they are also exposed to mechanical shear during injection. Not only so, chemical or enzymatic crosslinking during *in situ* gelation of hydrogel could also impose damage to cells within. For drug screening, biomaterial-assisted cell cultures face problems with uniformity, controllability and throughput. Using hydrogels, cells are typically involved during gelation, by which the process may affect cell viability and function. Gelation during cell seeding also hampers usage by most high-throughput equipment, since the hydrogel may need to be kept on ice to prevent gelation before cell seeding, and the hydrogel might jam dispensing tips, which are usually very thin to ensure accuracy for high-throughput screening. Pre-formed scaffolds could potentially separate biomaterial fabrication procedures from cell culture, however most scaffold-based products are available as bulk materials with relatively lower throughput<sup>14</sup>.

To overcome some of the shortcomings of current 3D culture methods, we have developed a microfabrication-cryogelation integrated technology to fabricate an off-the-shelf and user-friendly microcryogel array chip<sup>15</sup>. In this protocol, gelatin is selected to exemplify the microcryogel

fabrication technique as it is biocompatible, degradable, cost-effective, and no further modification is required for cell attachment. Other polymers of natural or synthetic sources could also be used for fabrication, depending on the application. Via this technology, we can fabricate miniaturized and highly elastic microcryogels with controllable size, shape and layout. When loaded with a variety of cell types, 3D microtissues could be formed for various applications. These unique features enable desired injectability, cell protection and site-directed retention after injection *in vivo* for enhanced therapeutic effects. Not only so, the microcryogels could be further processed to form 3D microtissue arrays that are compatible with common laboratory equipment and instruments to realize high-throughput cell culture for versatile drug screening and other cellular assays. Herein, we shall detail the fabrication process of microcryogels and its post-treatment as individual 3D microtissues or 3D microtissue arrays for two important applications, cell therapy and drug screening, respectively<sup>10,15</sup>.

## Protocol

Animal experiments followed strict protocol approved by the Animal Ethics Committee on the Center of Biomedical Analysis, Tsinghua University. Under approval of Ethics Committee, human adipose tissue was obtained from Department of Plastic Surgery of Peking Union Hospital with informed consent from the patients.

## 1. Fabrication of 3D Microcryogels

### 1. Design and fabrication of microstencil array chips

1. Use a commercial software to design arrays of specific geometries, such as circles, ellipses, triangles or clovers<sup>14</sup>, depending on subsequent application.  
NOTE: Refer to section 2 of the protocol for regenerative medicine and section 3 of protocol for drug screening for design details.
2. Import the design into the laser engraving software accompanying the laser engraving machine. Using the laser settings according to the factory recommendations for the laser engraving machine, laser-engrave the imported design onto Poly (methymethacrylate) (PMMA) sheets.
3. Wash the microstencil array chips with deionized water to clean debris from the laser engraving. Dry the microstencil array chips at 60 °C. Store in a sealed bag at room temperature for months.

### 2. Fabrication of microcryogel array chips

1. Place 4 microstencil array chips on the sample tray and insert into the plasma cleaner. Close the door of the cleaner and turn on the vacuum pump for 2 min, then turn on the maximum RF power (18 W) to treat the microstencil array chips in the plasma cleaner for 3 min at room temperature to increase hydrophilicity.
2. Add 0.06 g gelatin to 1 mL deionized water to form 6% (wt/vol) gelatin precursor solution (enough to make 5 chips). Warm at 60 °C in a water bath to dissolve adequately. Incubate on ice for 5 min.
3. Add 3  $\mu$ L of glutaraldehyde into the gelatin precursor solution to a final concentration of 0.3%. Mix thoroughly.
4. Pipette 200  $\mu$ L precursor solution with glutaraldehyde onto the upper surface of the microstencil array chip.  
NOTE: 200  $\mu$ L is sufficient for a 75 mm  $\times$  25 mm chip regardless of design. Increase the amount proportionally when surface area of chip is increased.
5. Manually distribute the solution evenly over the chip by scraping back and forth with a bent glass rod 2 to 3 times.  
NOTE: Each micro-well on the microstencil chip can be filled with precursor solution due to their hydrophilic nature after plasma treatment.
6. Immediately place the precursor-solution-filled array chip in a -20 °C freezer for 16 h for cryogelation.
7. Adjust the lyophilizer to -40 °C for 30 min. Place the array chips after cryogelation in the lyophilizer and lyophilize the array chips for 2 h in vacuum.  
NOTE: Gelatin microcryogels with interconnected macropores are formed because ice formed during cryogelation sublimates in the lyophilizer.
8. Proceed to section 2 for treatment of critical limb ischemia (CLI) and section 3 for high-throughput drug screening.

## 2. Harvesting Individual Microcryogels to Form Injectable 3D Microtissues for Treatment of CLI

### 1. Harvesting individual microcryogels

1. Design arrays (75 mm  $\times$  25 mm) of 600 circles, each with 400  $\mu$ m diameter, in commercial software for injectable 3D microtissue construction. Use PMMA of 300  $\mu$ m thickness for fabrication of microstencil array chip as detailed in section 1.1.
2. Fabricate microcryogel array chips as in section 1.2.
3. Fabricate a PDMS Ejector Pin array with the same design as in step 2.1.1 by standard soft lithography<sup>16,17</sup>.
4. Overlay the microcryogel array chip on top of the PDMS Ejector Pin array, aligning each microcryogel with an ejector pin on the array. Press the microcryogel array chip towards the ejector pin array to push the microcryogels out of the microwells with the protruding pins on the PDMS ejector pin array to harvest individual microcryogels.
5. Harvest the microcryogel into water and collect them with the aid of cell strainers. Use one strainer to collect microcryogels from one chip (*i.e.*, 600 microcryogels).
6. Wash microcryogels with 0.1 M NaBH<sub>4</sub> on ice for 20 min to quench any uncross-linked aldehyde residue. Use 5 mL of 0.1 M NaBH<sub>4</sub> per chip. Discard NaBH<sub>4</sub> and wash with 5 mL deionized water for 3 to 5 times, 15 min each time.
7. Discard water from the cell strainer and gather microcryogels into one cluster per cell strainer and place one cluster in one 35-mm Petri dish using a curved tweezer. Add 50 - 70  $\mu$ L deionized water to each cluster and cover the lid of the Petri dish. Gently tap the Petri dish on the tabletop to level out all microcryogels, so that no microcryogels are lying on top of another microcryogel to form a monolayer of microcryogels on the surface of the Petri dish.

8. Freeze the harvested microcryogels at  $-20\text{ }^{\circ}\text{C}$  for 4 to 16 h before lyophilizing them for 2 h (see step 1.2.7). Store microcryogels in a vacuum at room temperature until further use.

## 2. Characterization of microcryogels

1. Evaluate the pores of the microcryogels by scanning electron microscopy (SEM) imaging.
  1. Immobilize the harvested and lyophilized microcryogels onto a sample holder by double-side adhesive tape and coat with gold with a sputter coater for 90 s, before imaging by SEM<sup>11</sup>. Evaluate and analyze the distribution of diameters of pores in the microcryogel from seven different SEM images using image analysis software.
2. Weigh one cluster of 600 lyophilized microcryogels in a 35-mm Petri dish for the weight of dried gelatin microcryogels (GMs). Add 60  $\mu\text{L}$  deionized water to the cluster of lyophilized microcryogels and wait for 30 s for microcryogels to fully absorb water and swell. Weigh the swollen microcryogels.
  1. Determine the equilibrium swelling ratio and porosity of microcryogels, as the ratio of weight of swollen microcryogels to that of dried gelatin microcryogels and the ratio of weight of held water in microcryogels to that of hydrated microcryogels, respectively<sup>13</sup>.
3. Measure injectability of microcryogels using a programmable syringe pump integrated with a digital force gauge<sup>14</sup>.
  1. Stain 600 pieces of microcryogels by Trypan blue and suspend in 600  $\mu\text{L}$  15% gelatin solution to achieve homogeneous distribution. Load 1 mL microcryogel suspension in 1 mL syringe. Inject the mixture through a 27-gauge needle attached to the 1 mL syringe using a programmable syringe pump at flow rate of 1 mL/min.
  2. Monitor real-time injection force by digital force gauge testing and plot the force-time curve. After injection, observe the integrity of microcryogels under a microscope.  
NOTE: GMs suspended in 15% (wt/vol) gelatin solution can be smoothly injected and remained intact after injection.
4. Characterize the degradability of microcryogels.
  1. First, measure the weight of one cluster of 600 lyophilized microcryogels in a 35-mm Petri dish as the dry weight. Then, immerse 600 lyophilized microcryogels in 2 mL 0.025% (vol/vol) Trypsin/EDTA.
  2. Collect microcryogels from the solution using a cell strainer at different time points (*i.e.*, 10, 20, 30, 40, 50, 60, and 70 min). Wick away excess solution with a tissue. Measure the weight of microcryogels at different time points and calculate the degradation degree, as the ratio of weight of microcryogel at a certain time point to that of microcryogel at time zero.

## 3. Autoloading of cells into microcryogels to form 3D microtissues

1. Sterilize microcryogels from step 2.1.8 by ethylene oxide sterilization system with 12 h gas exposure followed by 12 h degassing under vacuum.
2. Choose human adipose-derived mesenchymal stromal cells (hMSCs) for treatment of mouse ischemic hindlimb. Isolate cells by following procedures as previously reported<sup>18</sup>.
3. Culture hMSCs in the growth medium containing 2% fetal bovine serum (FBS), 10 ng/mL epidermal growth factor (EGF), 10 ng/mL platelet-derived growth factor bb (PDGF-bb), 1X insulin transferrin selenium (ITS),  $10^{-8}$  M dexamethasone,  $10^{-4}$  M ascorbic acid 2-phosphate, 100 U/mL penicillin, and 100  $\mu\text{g}/\text{mL}$  streptomycin in DMEM/F12. Passage the cells at the ratio of 1:3 when confluent. Use cells of passage 3 to 5 in the following experiments.
4. Harvest hMSCs with trypsin and quantify the cell number using a Fuchs-Rosenthal counting chamber and resuspend to a density of  $8 \times 10^6$  cells/mL in hMSCs growth medium.
5. Pipette 60  $\mu\text{L}$  hMSCs suspension onto the monolayer of 600 microcryogels with diameter of 400  $\mu\text{m}$  in a 35-mm dish from section 2.1. Cells are automatically absorbed into the porous micro-structures of the microcryogels.
6. Maintain in a humidified chamber and incubate at  $37\text{ }^{\circ}\text{C}$  for 2 h to allow cells to attach. After 2 h of incubation, add 2 mL culture medium. Change the medium every 2 days. Culture hMSCs-loaded microcryogels for 2 days to form 3D microtissues.
7. After 2 days culturing, pipette 100 hMSCs-loaded microcryogels per well on a 96-well plate, add 120  $\mu\text{L}$  of resazurin working solution prepared according to the manufacturer's instruction into each well. Incubate for 2 h at  $37\text{ }^{\circ}\text{C}$ .
  1. Detect fluorescence of resazurin metabolized by viable cells in a microplate reader with an excitation light wavelength of 560 nm and emission light wavelength of 590 nm. Establish a standard curve of cell number vs. fluorescence using hMSCs to interpolate cell number from fluorescence intensity for future experiment according to the kit protocol<sup>13</sup>.
8. Assess number of hMSCs in microcryogels from day 0 to day 4 using resazurin as described in step 2.3.7 from day 0 to day 4.
9. Stain cells in microcryogels with 1:500 dilution of Calcein AM and 1:250 dilution of Propidium Iodide (known as live/dead staining) in phosphate buffered saline (PBS) and observe under fluorescence microscope or confocal fluorescence microscope.

## 4. Injection of 3D microtissues *in vivo* for treatment of CLI in mouse model

1. Establish critical hindlimb ischemia of female BALB/c nude mice as reported<sup>11,19</sup> to determine the therapeutic effect of 3D microtissue-based therapy.
2. Transfer the microtissues from step 2.3.6 using a 5-mL pipette into a cell strainer and filter away the culture medium.
3. Resuspend the hMSCs-loaded 3D microtissues in 15% gelatin solution, at a density of 100 microcryogels per 100  $\mu\text{L}$  solution.
4. Before surgery, sterilize surgical tools by autoclave and perform surgery in an animal operating room in an Animal Facility Center.
5. Place the mouse into the anesthesia induction chamber containing 1-3% isoflurane in 100% oxygen at a flow rate of 1 L/min. Apply erythromycin on the eyes of the mouse to prevent drying. Through a 1-cm-long skin incision, ligate the femoral artery and its branches with 5-10 silk sutures and excise<sup>19</sup>.
6. Inject indocyanine green (ICG) (0.1 mL of 100  $\mu\text{g}/\text{mL}$ ) through the tail vein injection to monitor blood flow. Perform ICG fluorescence imaging using a fluorescence imaging system (here, homemade system) in the reflectance geometry<sup>11</sup>.
7. Intramuscularly inject microtissues into three sites of the gracilis muscle around the artery incision using a 1 mL syringe with a 23-gauge needle.

8. After surgery, keep the mouse warm with a heated pad in the recovery cage. Inject subcutaneously meloxicam to relieve the pain and monitor continuously until awake.
9. After 28 days, monitor the therapeutic efficacy of 3D microtissue-treated limb by fluorescence imaging<sup>11</sup>.  
Note: Inject subcutaneously meloxicam to relieve the pain when the mouse showed spontaneous limb amputation.
10. Euthanize mice with carbon dioxide after completion of experiments.  
NOTE: Here, euthanasia with carbon dioxide was performed according to strict protocol approved by the Animal Ethics Committee on the Center of Biomedical Analysis, Tsinghua University.

### 3. Assembly of Microtissue Array Chip for High-throughput Drug Screening

#### 1. Assembly of microcryogel array for on-chip cell culture

1. Modify the design in section 1.1 according to conventional multi-well plate dimensions, *i.e.*, for 384-multi-well format, design an array of 16 × 24 wells (row by column), each of 2 mm diameter and 4.5 mm center-to-center spacing.
2. Laser engrave onto a 500 μm thick PMMA sheet as described in section 1.1.
3. Fabricate microcryogels as described in section 1.2 using the 384-multi-well array chip obtained from step 3.1.2. This microcryogel-containing array is designated as the microcryogel array chip.
4. Wash the microcryogel array chip with 50 mL 0.1 M NaBH<sub>4</sub> to quench any residual aldehyde uncross-linked, then repeatedly rinse with 50 mL deionized water for 3 times, 2 h each time.
5. Discard the water, freeze the microcryogel array chip at -20 °C for 4 to 16 h before lyophilizing according to step 1.2.7.
6. Modify the 384-multi-well array design in step 3.1.1 to contain 16 × 24 wells, each of 3 mm diameter and 4.5 mm center-to-center spacing.
7. Remove one side of the backing from a sheet of ultra-thin (10 μm) biocompatible double-sided adhesive tape and paste it to one side of a piece of 3-mm-thick PMMA sheet. Laser engrave the design from step 3.1.4 onto this 3-mm-thick PMMA sheet according to section 1.1. This array is designated as the reservoir array.
8. Align the microcryogel array chip with the reservoir array chip and adhere together tightly to assemble the 3D microcryogel array chip for on-chip cell culture. Sterilize by ultra-violet radiation for 1 h.
9. Store 3D microcryogel array chips in vacuum at room temperature for further experiments.

#### 2. Drug screening on 3D microtissue arrays

1. Fill up a wet box with 25 mL sterile de-ionized water to serve as a humidity chamber for cell culture. Pre-heat in a humidified 5% CO<sub>2</sub> incubator to 37 °C.
2. Harvest non-small-cell lung cancer cells (NCI-H460) and hepatocellular carcinoma cells (HepG2) from the tissue culture plates according to standard protocol and re-suspend in culture media to a final density of 1.0 × 10<sup>6</sup> cells/mL. Mix thoroughly.  
NOTE: RPM1640 with 10% FBS, 100 U/mL penicillin and 100 μg/mL streptomycin is used for NCI-H460. Use DMEM with 10% FBS, 100 U/mL penicillin and 100 μg/mL streptomycin for HepG2.
3. Remove the humidity chamber from incubator. Use tweezers to carefully place the assembled 3D microcryogel array chip from step 3.1.9 in the humidity chamber. Take caution not to wet the microcryogels with water in the chamber.
4. Mix the cell suspension thoroughly, then aliquot 3 μL of cell suspension directly onto the microcryogel into each well.  
NOTE: The pipette tip should lightly touch the surface of the microcryogel before expelling cell suspension. Cells are auto-loaded into the microcryogel by absorption. Do not seed cells in the peripheral wells.
5. Add 10 μL of media to each well after cells are seeded into microcryogel using multi-channel pipette, such as a 96-channel liquid handler. Medium is also added to peripheral wells.  
NOTE: Use RPM1640 media with 10% FBS, 100 U/mL penicillin and 100 μg/mL streptomycin for H460 cells. Use DMEM media with 10% FBS, 100 U/mL penicillin and 100 μg/mL streptomycin for HepaG2 cells.
6. Culture the cell-loaded microcryogel array chip in the humidity chamber for 24 h in a humidified 5% CO<sub>2</sub> incubator at 37 °C to form 3D microtissue array.
7. Dissolve doxorubicin and IMMLG-8439<sup>9</sup> in dimethyl sulfoxide (DMSO) to form a stock solution of 10 mM. Dilute drugs with culture medium to form a 10-fold dilution concentration gradient from 2 nM to 200 μM.
8. Add 10 μL of drug solutions into each well. Use 0.1% DMSO (diluted in medium) as the control. Incubate the drug loaded 3D microtissue array in a humidified 5% CO<sub>2</sub> incubator at 37 °C for 24 h.
9. Add 4 μL of resazurin stock solution to each well. Incubate at 37 °C for 2 h. Place the 3D microtissue array in the microplate reader and detect fluorescence of resazurin metabolized by viable cells at an excitation light wavelength of 560 nm and emission light wavelength of 590 nm.
10. Subtract the resazurin baseline signal from all wells before further data processing. Calculate the cell viability fraction of each well by dividing its fluorescence signal by the average fluorescence signal of the control wells.
11. Plot the dose-response curve in plotting software with the cell viability fraction as the Y-axis and the base 10 logarithm of drug concentration as the X-axis. Interpolate the 50% inhibition concentration (IC<sub>50</sub>) at the cell viability fraction of 0.5.

## Representative Results

### Fabrication and characterization of microcryogels for 3D microtissue formation.

According to this protocol, microcryogels were fabricated to form the 3D microtissues and individual microcryogels or microcryogel arrays, and were applied to regenerative therapy and drug screening, respectively (**Figure 1**). Microstencil array chips fabricated from PMMA were applied as micromolds for microcryogel array chips. Variable geometrical designs could be prepared for the microstencil array chip. We chose a representative 45 mm x 14 mm microstencil array chip as an example, which contained various shapes (*i.e.*, circle, ellipse, triangle, and clover) and a circle-shaped microstencil array chip with different sizes (diameters = 100, 200, 400 and 800  $\mu\text{m}$ ). To enhance the visibility of micromolds on the array chips, light epi-illumination images were observed (**Figure 2A, B**). Microcryogels harvested from the array chips exhibited desired shapes and sizes (**Figure 2C, D**). Such microcryogels with desired geometrical features could possibly be applied as templates to form different cellular units that mimic certain architectures of native tissues. The harvested GMs (gelatin microcryogels) had pre-defined shapes and sizes (**Figure 3A**). SEM observation demonstrated that microcryogels contained interconnected macroporous structures with pore sizes in the range of 30 - 80  $\mu\text{m}$  (**Figure 3B**).

### Enhanced injectability of hMSCs-loaded microtissues for improved ischemic limb salvage

Using the programmable syringe pump integrated with a digital force gauge<sup>14</sup>, the injectability of GMs was quantitatively assessed. At a flow rate of 1 mL/min, the GMs with a density of 1,000 microcryogels per mL were injected under 6 N, which was lower than the clinically acceptable force of 10 N<sup>20</sup> (**Figure 3F**). Basing on cell protection enabled by GMs, hMSCs in GMs had high viability and maintained great proliferative capacity after injection during 5 days of culture (**Figure 3H**).

The mouse limb ischemia model was chosen to assess the therapeutic efficacy of the injectable hMSC-loaded microtissues. Physiological status of ischemic limbs was examined 28 days after surgery (**Figure 4A**). No limb salvage was observed in the sham group or GMs control group. In the 10<sup>5</sup> free cell treatment group, 50% total toe amputation, 25% partial toe amputation, and 25% partial limb amputation were observed within 7 days, resulting in 80% limb loss and 20% total toe amputation after 28 days. In contrast, microtissues treatment with 10<sup>5</sup> hMSCs achieved improved limb salvage (75%) with only 25% mice showed spontaneous toe amputation after 28 days. 10<sup>6</sup> hMSCs, the minimum effective cell number used in most previous studies, was chosen as the positive control<sup>21</sup>. Only 2 of the 4 mice showed limb salvage, but all had minor necrosis.

Blood perfusion was monitored and assessed in the aid of indocyanine green (ICG), an FDA approved angiographic contrast agent. The result showed that fluorescence signals appeared in the microtissue-treated mice and in the 10<sup>6</sup> free hMSCs-treated mice. There is no evident fluorescence signal in the ischemic hindlimbs in the sham or GM group until day 28 (**Figure 4B**).

These results further confirmed that 3D microtissue-assisted hMSCs therapy achieved superior therapeutic effects for CLI treatment which represents the minimum effective dosage for cell-based therapy in the mouse model so far.

### High-throughput drug cytotoxicity screening on 3D microtissue array chip

A ready-to-use 3D microcryogel array for on-chip cell culture could be easily fabricated by retaining microcryogels on the PMMA chip after lyophilization and combining with the corresponding well-array chip with biocompatible adhesive tapes (**Figure 1** and **Figure 5A**). In this two-part cell culture array, the top well-array chip served as reservoirs for the culture medium, drug solutions and assay reagents, while the cells were cultured in the 3D microcryogel immobilized on the bottom array chip. The adhesive tapes between the top and bottom array chip allowed generation of 384 individual wells for high-throughput 3D cell culture (**Figure 5B**), hence providing a practical tool for drug discovery.

As described in the protocol, 3D microtissue array was formed by directly seeding cells into microcryogels before adding medium to the reservoirs. Using RFP-labeled NIH-3T3 cells, we demonstrated that the cells were uniformly distributed with multi-layers within the 3D architecture of microcryogels (**Figure 5C, D**). SEM images showed that cells adhered firmly to the walls of the pores and even exhibited extended filopodia along or across adjacent walls of macropores in the microcryogels (**Figure 5E**).

We then showed the feasibility of applying this 3D microtissue array for high-throughput drug testing using two cancer cell lines and two compounds. Hepatocellular carcinoma cells (HepG2) were treated with Doxorubicin while non-small-cell lung cancer cells (NCI-H460) were treated with IMMLG-8439, a new tumor inhibitor. Five to nine discrete concentrations of each drug were administered to six adjacent wells as replicates, with 0.1% DMSO in culture medium as the negative control. A cytotoxicity assay was similarly performed for cells cultured in traditional 2D multi-well plates. After 24 h of incubation, the cell viability assay was used to assess the drug responses of cells in both 2D and 3D. Drug response curves were plotted using normalized cell viability rates at different drug concentrations, and the IC50 was then interpolated from these curves. A higher IC50 value would indicate that cells are more drug-resistant. From **Figure 5F** and **5I**, we observed a significant increase in drug resistance when cells were cultured on 3D microtissue array than in 2D. The IC50 of Doxorubicin against HepG2 cells reached 165.959  $\mu\text{M}$ , relative to 18.239 nM on 2D; the IC50 of IMMLG-8439 on NCI-H460 cells was similarly elevated to 331.894 nM in 3D while only requiring 1.294 nM on 2D. Such observation was in concordance with reports of increased drug resistance in 3D culture over 2D culture by other researchers<sup>22,23</sup>.

We attributed such increase in drug resistance to the complexity of the 3D microenvironment compared to the planar configuration of 2D culture. SEM images revealed that HepG2 cells gathered as spheroids decorating the surfaces of macropores in the microcryogel. These cells are tightly clustered and such enhanced cell-cell interaction could be a source of drug resistance in HepG2<sup>22</sup>. It was also interesting to note that these cell clusters were not freely suspended spheroids as they still maintained some adhesion to the matrix (**Figure 5G, H**). Conversely, epithelial-mesenchymal-transition (EMT) was speculated to have occurred when the non-small lung cancer cells, NCI-H460, were cultured on 3D microcryogels. NCJ-H460 cells spread out like fibroblasts (**Figure 5J, K**) instead of clustering like HepG2. Hence, we speculated that the increase in drug resistance could be a result from a transition of epithelial NCI-H460 cells to a more malignant state<sup>18,19,20,21,22,23</sup>.

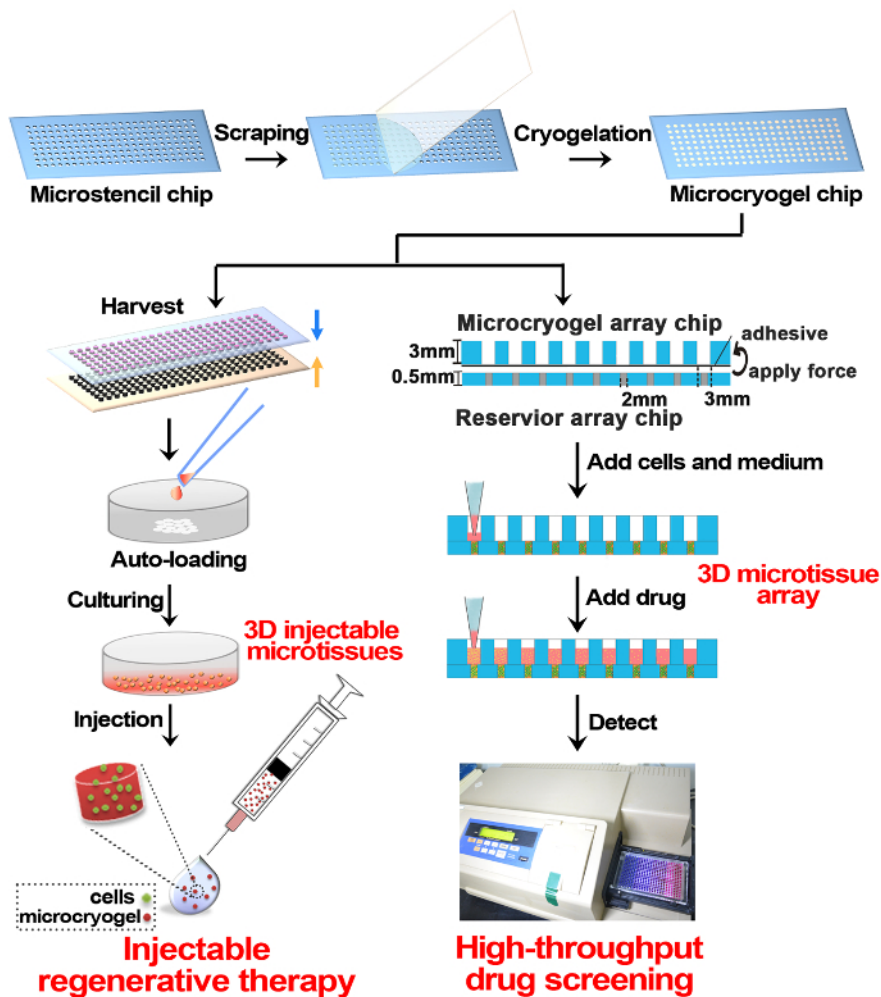


**Figure 1: Schematic of 3D Microtissue Fabrication and Application in Regenerative Therapy and Drug Screening.** Briefly, size and shape-controllable microcryogel chip was fabricated on an array PMMA chip by cryogelation of gelatin. The microcryogel chips can be harvested off-chip as individual microcryogels and further, individual microcryogels can be auto-loaded with cells and cultured to form 3D microtissues for injectable regenerative therapy. Another application of microcryogel chips is to assemble with a reservoir array chip and then further, load cells and culture into 3D microtissue arrays for high-throughput drug screening. [Please click here to view a larger version of this figure.](#)

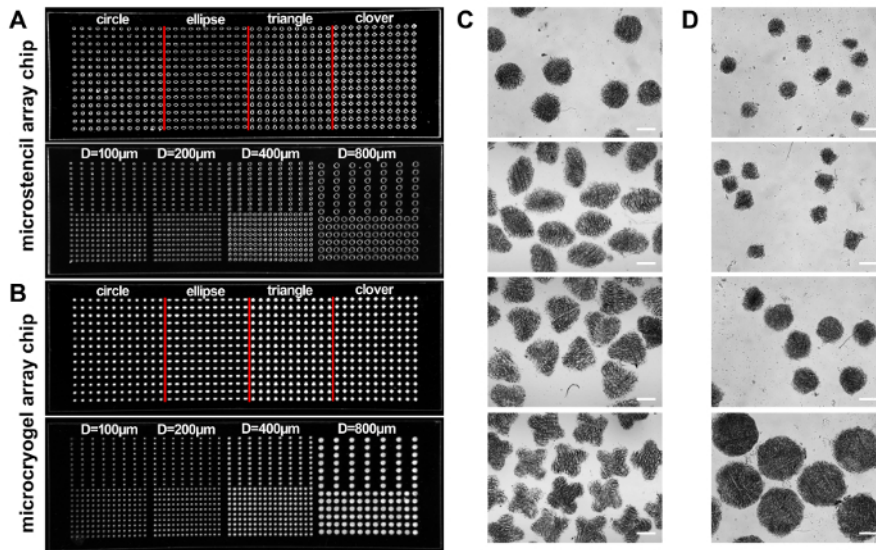


**Figure 2: Microstencil Array Chips.** (A, B) Photographs of two PMMA microstencil chips containing arrayed microwells with different shapes (*i.e.*, circle, ellipse, triangle and clover) and circular shape with different sizes (diameter: 100, 200, 400 and 800  $\mu\text{m}$ ), respectively (A), and two corresponding microcryogel array chips (B). (C, D) Microscopic images of the individual microcryogels harvested from the two microcryogels array chips. Scale bar = 500  $\mu\text{m}$ . This figure has been modified with permission from reference<sup>14</sup>. [Please click here to view a larger version of this figure.](#)

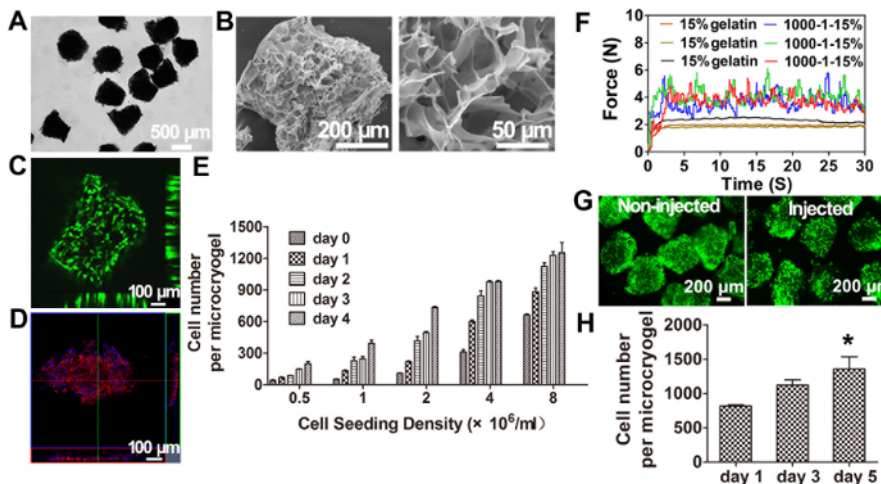


**Figure 3: Characterization of 3D Injectable Microtissues.** (A) Photographs of harvested microcryogels. (B) Scanning electron micrograph (SEM) images of microcryogels showing interconnected and macroporous structures. (C, D) Fluorescence microscopic and 3D reconstructed confocal images of hMSCs-loaded microtissues stained by live/dead and rhodamine phalloidin. (E) Quantification of hMSCs autoloading and proliferation in GMs with different initial loading densities. (F) Real-time injection force measurement curves for triple injections of 1,000 GMs in 1 mL of 15% (wt/vol) gelatin solution at 1 mL/min injection rate (1,000-1-15%). (G) Live/dead cell viability assay of hMSCs-loaded microtissues pre-injection and post-injection. (H) Proliferation of hMSCs loaded in GMs post-injection after 1, 3, and 5 days of culture ( $n = 3$ ).  $*p < 0.05$ , one-way ANOVA compared to day 1. Data are presented as mean  $\pm$  SEM. This figure has been modified with permission from reference<sup>11</sup>. [Please click here to view a larger version of this figure.](#)

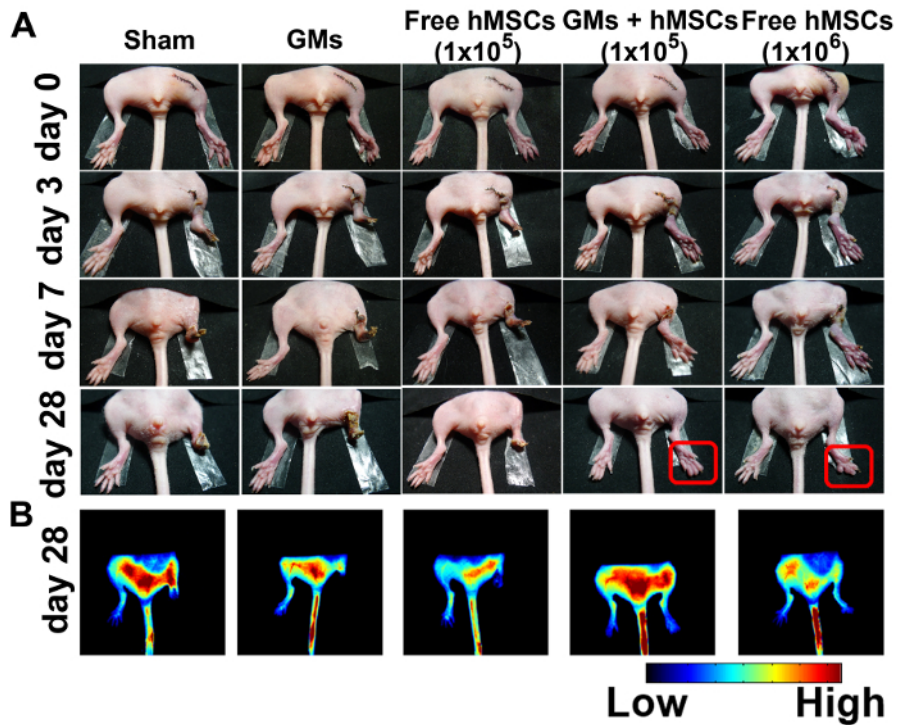


**Figure 4: Improved Salvage and Enhanced Angiogenesis in Ischemic Hindlimbs Treated with 3D Injectable Microtissues. (A)** Representative photographs of sham ( $n = 4$ ), blank microcryogels ( $n = 4$ ), free hMSCs ( $10^5$ ) ( $n = 8$ ), hMSCs ( $10^5$ )-loaded microtissues ( $n = 8$ ), and free hMSCs ( $10^6$ ) ( $n = 4$ ) at 0, 3, 7, and 28 day after treatment. **(B)** Fluorescence images obtained 100 s after ICG injection on day 28. This figure has been modified with permission from reference<sup>11</sup>. [Please click here to view a larger version of this figure.](#)



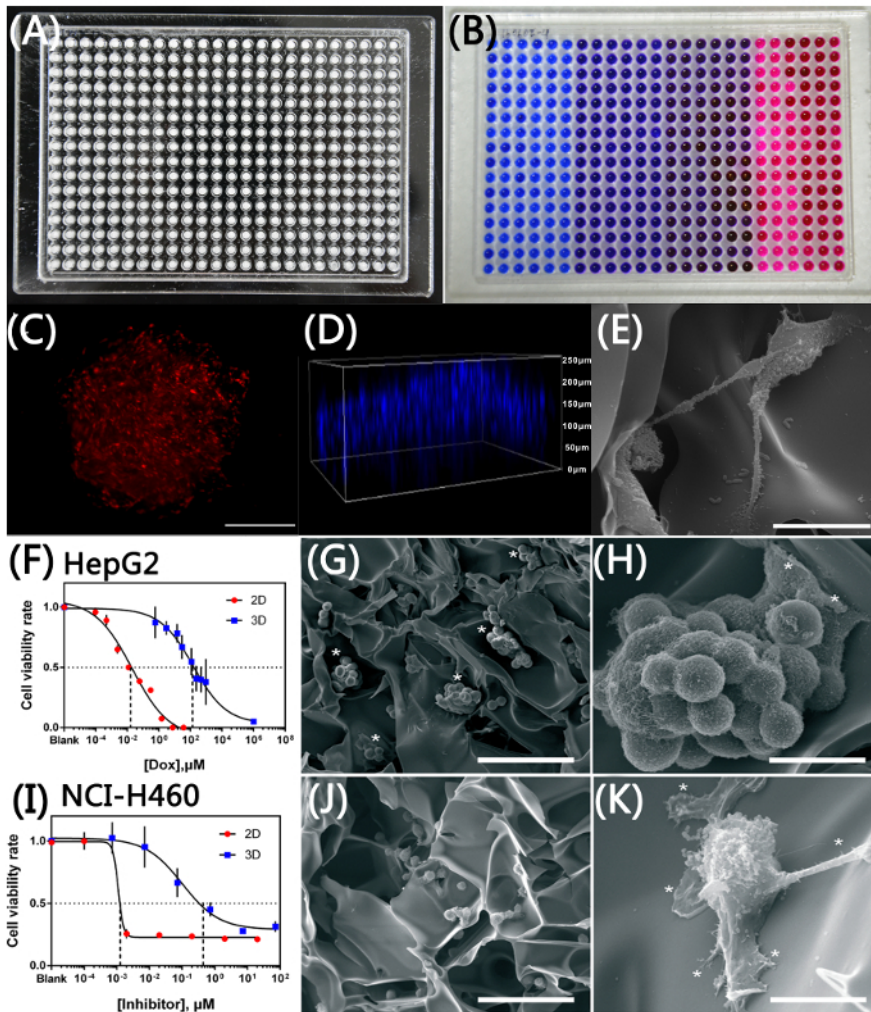


**Figure 5: 3D Microtissue Array for High-throughput Drug Screening.** (A) Photograph of 3D microtissue array in 384-multi-well format after assembly, and (B) resazurin cell viability assay performed on the array. (C) RFP-3T3 cells within microcryogel post-seeding (scale bar = 200  $\mu\text{m}$ ). (D) 3D reconstruction of nuclei staining depicting homogeneous distribution of cells in multi-layers in microcryogel. (E) Scanning electron micrograph image of RFP-3T3 cells spreading extensively on macroporous walls in microcryogels (scale bar = 20  $\mu\text{m}$ ). Cytotoxicity testing of (F) doxorubicin on HepG2 cells and (I) IMMLG-8439 on NCI-H460 cells in 3D microtissue array showing increased IC<sub>50</sub> comparing to their 2D counterparts. Data are shown as mean  $\pm$  SD. (G) Small spheroids of HepG2 cells in microcryogel (scale bar = 100  $\mu\text{m}$ ), with (asterisks in H) partial adherence on the microcryogel wall (scale bar = 20  $\mu\text{m}$ ). (J) NCI-H460 cells adhered and spread within the microcryogel (scale bar = 100  $\mu\text{m}$ ). (K) NCI-H460 cells exhibiting fibroblastic morphology (scale bar = 20  $\mu\text{m}$ ). This figure has been modified with permission from reference<sup>9</sup>. Please click here to view a larger version of this figure.

## Discussion

Regenerative medicine and *in vitro* models for drug screening are two important applications for tissue engineering<sup>5,6,7,8,9</sup>. While these two applications have vastly different needs, a common ground between them lies in the need for a more biomimetic culturing condition to enhance cell functions<sup>19</sup>. Only with improved cell functions in research can we treat diseases better<sup>20,21</sup>, and if cultured cells reflect drug responses more accurately can we accelerate drug discovery<sup>6,7</sup>. Cell survival after engraftment *in vivo* is a crucial requirement for regenerative medicine, while throughput is important for drug screening to handle thousands of compounds at one time. These two requirements are specific to their respective applications, and seldom can one technology meet both requirements. Thus, we have uniquely integrated microfabrication technology with cryogel preparation to produce macroporous microcryogels, which could be harvested off-chip as individual cell-loaded carriers for regenerative therapy, or retained on chip for further assembly into array for high-throughput drug screening. The microscale and macroporosity of these novel microcryogels allow automatic and homogeneous loading of cells by simple absorption. Using novel microstencil fabrication of microcryogel array chips, hundreds and thousands of microscale cryogels with uniform and reproducible geometrical features could be easily and efficiently generated. The microcryogels could be prepared and stored by vacuum packaging as an off-the-shelf, ready-to-use product to facilitate preparation of 3D microtissues in common laboratories for subsequent applications. Using this fabrication technique, we were able to meet both the common ground (3D culture condition for better biomimicry) and specific requirements for the two different applications (elasticity to protect cells during injection for regenerative medicine and high-throughput in an array format for drug screening).

Cell-based therapy holds great promise for repair of various damaged tissues or organs<sup>24</sup>. However, cell retention, cell survival, and reproducibility of the treatment are still poor due to mechanical damage during injection, high leakage to surrounding tissues, and ischemia and inflammation in the *in vivo* environment within the lesion tissues<sup>25</sup>. Some researchers have used preformed cellular aggregates to improve free cell injection. However, it requires a large amount of cells to form cell aggregates, which leads to high cost, non-uniform size, and uncontrollable aggregate numbers<sup>26</sup>. Moreover, mechanical injury and cell death are still inevitable during injection. Alternatively, biomaterial-assisted cell therapy has been developed in which responsive biomaterials (e.g., thermal or pH-sensitive hydrogel) can be mixed with cells and gelation *in situ* to realize cell retention<sup>27</sup>. However, *in situ* cross-linked biomaterials do not allow priming of cells *in vitro* and result in immediate exposure of cells to an ischemic and inflammatory microenvironment at the lesion site. It is urgent to solve these problems to enhance therapeutic efficiency. A major advantage of microcryogels fabricated using this protocol is their desired injectability as a result of their miniaturized size and exceptional elasticity, facilitating their application in cell delivery. The injectability of microcryogels enables cell protection during cell delivery, hence they could be constituted into 3D injectable microtissues after *in vitro* priming of cells in the microcryogel to enhance both extracellular matrix (ECM) protein deposition as well as cell-cell interactions. The 3D injectable microtissues result in microscale tissue-like ensembles representing an optimal delivery strategy to facilitate cell protection, engraftment, survival, and hence improve the ultimate therapeutic effects at the lesion site.

Besides enhanced therapeutic effects for cell therapy, our results were also indicative of the complex impact of 3D microenvironment on cellular drug responses. Utilizing biomimicking culture conditions, it would be possible to elicit *in vitro* cellular drug responses more representative of *in vivo* responses, hence accelerating drug discovery<sup>6,7,28</sup>. Spheroids are popular choice of 3D cell culture configuration and many techniques have been developed to assist researchers generate spheroids. Low-adhesive tissue culture plates<sup>29</sup> or plate surfaces that are modified with nano-imprints<sup>8</sup> were also used to coerce cells to aggregate by preventing cell-matrix adhesion. While these techniques are relatively simple to use, problems such as loss of spheroids during medium exchange and other operations as well as size variability of spheroids are problems hindering large-scale adoption of such technology<sup>6</sup>. More homogeneous spheroids could be formed using hanging drop<sup>30,31,32,33</sup>, however it is labor intensive if not using specialized plates. Using specialized multi-well hanging drop plates, and integrating with automated liquid handling systems<sup>6,31</sup>, high-throughput screening could be realized. The largest drawback of spheroid culture is the lack of ECM, which has been identified to play vital roles in all physiological and pathological tissue developments<sup>34</sup>. A brain model study revealed that spheroids cultured inside an ECM scaffold, in comparison to pure spheroids, had increased drug resistance, enhanced acidosis due to higher lactate production and improved angiogenesis with increasing expression of related factors<sup>34</sup>. Other studies have also shown that presence of matrix could provide necessary mechano-signaling to promote EMT and supports recapitulation of tumor features such as invasion and metastasis<sup>3,35,36,37</sup>.

With increasing understanding of the importance of ECM in pathological development, there is no doubt that incorporating ECM into 3D culture methods could help mimic *in vivo* situations better<sup>6</sup>. Hydrogels of natural or synthetic materials have been applied to generate several *in vitro* 3D tumor models for assessment of chemotherapeutics due to their flexibility and controllability of biophysical properties (such as rigidity)<sup>38,39,40,41,42</sup>. While hydrogels with tunable biophysical properties had indeed modeled important biological features of tumor cells to facilitate more accurate drug screening, several disadvantages of this method have hindered its widespread use in drug screening. Crosslinking of polymers in the presence of cells is necessary to encapsulate cells within hydrogel matrix, which could potentially damage cells. Not only so, hydrogels of different biophysical properties present different challenges to cells encapsulated within. In soft hydrogels, high water content could support cell growth but such hydrogels degrade quickly, giving short-term support for 3D cell culture. On the other hand, stiffer hydrogels with high cross-linking could slow down degradation but low water content could not support cell growth and high crosslinker concentration usually induces high cytotoxicity<sup>43,44</sup>. Not only so, preparing 3D cell culture with hydrogels is labor-intensive and is not compatible with most high-throughput liquid handling systems as temperature control of hydrogel precursor solution is important and jamming of thin dispensing tips could result from gelation of hydrogel within the tips. These disadvantages have thus prompted the search for alternative ECM surrogates, *i.e.*, scaffold-based ECM<sup>34</sup>.

Using pre-formed scaffolds, cells could be exempted from the biomaterial fabrication process and hence provide the possibility for more control over scaffold fabrication as harsher conditions could be used without fear of damaging the cells. Several investigations have shown that the tumor cells cultured in 3D scaffolds display higher drug resistance compared with cells cultured in 2D due to increased malignancy and enhanced cell-ECM interaction<sup>45,46,47</sup>. Such observations are consistent with our results presented here. In our other works, we have further demonstrated the versatility of the 3D microtissue array and its advantages over the other techniques mentioned above. In a recent work, we were able to enhance hepatic function by promoting the epithelial phenotype of HepaRG cells by culturing on a 3D microtissue array and such array was applied to drug hepatotoxicity evaluation<sup>47</sup>. Owing to uniformity of pore sizes within the 3D macroporous scaffolds, we were able to control the size of liver cell spheroids to fall within 50-80  $\mu\text{m}$ , regardless of the initial cell-seeding density. This provides a significant advantage over free-forming spheroids with non-uniform sizes. Not only do spheroids grow uniformly within each scaffold, cells between wells are also uniformly seeded, giving Coefficient of Variation (CV) comparable with cells seeding in 2D (*i.e.*, CV = 0.09 in 3D microtissue array and CV = 0.05 in 2D commercial plate; data not shown). In another work, we have demonstrated that we were able to form liver microtumor on 3D microtissue array to recapitulate tumor-stromal interactions for screening of stroma-reprogrammed combinatorial therapy<sup>48</sup>. Liver microtumors were generated by long-term (5 days) co-culture of fibroblasts with tumor cells at high density. We observed barriers towards drug diffusion due to the compact cell and ECM structure formed in the liver microtumor, which was similarly observed *in vivo*<sup>32</sup>. Using luciferase-labeled cancer cells and mechanically-primed stromal cells, combined with luminescence of luciferin as the specific read-out for cancer cells, high-throughput screening of novel therapeutic agents or combinations against tumor-stromal interaction is made possible.

Despite the many unique advantages of our technique, a drawback of current microcryogels is non-transparency, hindering detailed optical observation of cells in microcryogels. Further improvements for these microcryogels would include fine-tuning their optical properties to enhance imaging of cells in microcryogels for observation. Also, important biophysical properties such as rigidity have not been explored in our technique, which would need to be addressed if we want to better mimic physiological and pathological tissues of different biophysical properties.

While our technique allows for simple generation of 3D microtissues, some cautions must be taken for successful experiments. When fabricating 3D microcryogels on microstencil array chip, it is important to ensure that the microcryogels remain frozen when placed in the lyophilizer. Hence it is essential to pre-cool the lyophilizer and to transfer microcryogels from the -20 °C freezer to the lyophilizer quickly. The melting of microcryogels before lyophilizing or during lyophilizing will cause pores to collapse and hence affect the porosity of microcryogels fabricated. When culturing 3D microtissues in the array format, attention is required to ensure the adhesiveness between the two arrays is sufficient to prevent cross-contamination between wells. Also, while miniaturizing cell culture has its advantage in increasing the throughput and reducing

reagent consumption, its drawback is that the low culture volume could not support long-term cell culture without frequent media replenishment. Not only so, it is critical to maintain the humidity of the culture environment to prevent influence on cell viability due to media evaporation, since only a few microliters of cell suspension or media is added. Evaporation will also affect the viability of cells in the peripheral wells, hence it is vital to avoid culturing cells in these wells.

Nonetheless, our robust technique provides an option to generate 3D microtissues in an easy-to-use manner, which could potentially make 3D culture a common cell manipulation method for most laboratories, to accelerate both basic and translational science advancements.

## Disclosures

The authors have nothing to disclose.

## Acknowledgements

This work was financially supported by the National Natural Science Foundation of China (Grants: 81522022, 51461165302). The authors would like to acknowledge all Du lab members for general assistance.

## References

1. Cukierman, E., Pankov, R., Stevens, D. R., & Yamada, K. M. Taking cell-matrix adhesions to the third dimension. *Science*. **294** (5547), 1708-1712 (2001).
2. Abbott, A. Cell culture: biology's new dimension. *Nature*. **424** (6951), 870-872 (2003).
3. Loessner, D. *et al.* Bioengineered 3D platform to explore cell-ECM interactions and drug resistance of epithelial ovarian cancer cells. *Biomaterials*. **31** (32), 8494-8506 (2010).
4. Fischbach, M. A., Bluestone, J. A., & Lim, W. A. Cell-based therapeutics: the next pillar of medicine. *Sci Transl Med*. **5** (179), 179ps177 (2013).
5. Kuraitis, D., Giordano, C., Ruel, M., Musaro, A., & Suuronen, E. J. Exploiting extracellular matrix-stem cell interactions: a review of natural materials for therapeutic muscle regeneration. *Biomaterials*. **33** (2), 428-443 (2012).
6. Breslin, S., & O'Driscoll, L. Three-dimensional cell culture: the missing link in drug discovery. *Drug Discov Today*. **18** (5-6), 240-249 (2013).
7. Lovitt, C. J., Shelper, T. B., & Avery, V. M. Miniaturized three-dimensional cancer model for drug evaluation. *Assay Drug Dev Technol*. **11** (7), 435-448 (2013).
8. Yoshii, Y. *et al.* High-throughput screening with nanoimprinting 3D culture for efficient drug development by mimicking the tumor environment. *Biomaterials*. **51** 278-289 (2015).
9. Li, X. *et al.* Micro-scaffold array chip for upgrading cell-based high-throughput drug testing to 3D using benchtop equipment. *Lab Chip*. **14** (3), 471-481 (2014).
10. Qi, C., Yan, X., Huang, C., Melerzanov, A., & Du, Y. Biomaterials as carrier, barrier and reactor for cell-based regenerative medicine. *Protein Cell*. **6** (9), 638-653 (2015).
11. Li, Y. *et al.* Primed 3D injectable microniches enabling low-dosage cell therapy for critical limb ischemia. *Proc Natl Acad Sci U S A*. **111** (37), 13511-13516 (2014).
12. Liu, W. *et al.* Magnetically controllable 3D microtissues based on magnetic microcryogels. *Lab Chip*. **14** (15), 2614-2625 (2014).
13. Zhao, S., Zhao, H., Zhang, X., Li, Y., & Du, Y. Off-the-shelf microsphere arrays for facile and efficient construction of miniaturized 3D cellular microenvironments for versatile cell-based assays. *Lab Chip*. **13** (12), 2350-2358 (2013).
14. Liu, W. *et al.* Microcryogels as injectable 3-D cellular microniches for site-directed and augmented cell delivery. *Acta Biomater*. **10** (5), 1864-1875 (2014).
15. Hakanson, M. *et al.* Controlled breast cancer microarrays for the deconvolution of cellular multilayering and density effects upon drug responses. *PLoS One*. **7** (6), e40141 (2012).
16. Du, Y. *et al.* Rapid generation of spatially and temporally controllable long-range concentration gradients in a microfluidic device. *Lab Chip*. **9** (6), 761-767 (2009).
17. He, J. *et al.* Microfluidic synthesis of composite cross-gradient materials for investigating cell-biomaterial interactions. *Biotechnol Bioeng*. **108** (1), 175-185 (2011).
18. Zeng, Y. *et al.* Preformed gelatin microcryogels as injectable cell carriers for enhanced skin wound healing. *Acta Biomater*. **25** 291-303 (2015).
19. Yang, F. *et al.* Genetic engineering of human stem cells for enhanced angiogenesis using biodegradable polymeric nanoparticles. *Proc Natl Acad Sci U S A*. **107** (8), 3317-3322 (2010).
20. Zhang, L. *et al.* Delayed administration of human umbilical tissue-derived cells improved neurological functional recovery in a rodent model of focal ischemia. *Stroke*. **42** (5), 1437-1444 (2011).
21. Kinnaird, T. *et al.* Local delivery of marrow-derived stromal cells augments collateral perfusion through paracrine mechanisms. *Circulation*. **109** (12), 1543-1549 (2004).
22. Fischbach, C. *et al.* Engineering tumors with 3D scaffolds. *Nat Methods*. **4** (10), 855-860 (2007).
23. Dhiman, H. K., Ray, A. R., & Panda, A. K. Three-dimensional chitosan scaffold-based MCF-7 cell culture for the determination of the cytotoxicity of tamoxifen. *Biomaterials*. **26** (9), 979-986 (2005).
24. Gimble, J. M., Guilak, F., & Bunnell, B. A. Clinical and preclinical translation of cell-based therapies using adipose tissue-derived cells. *Stem Cell Res Ther*. **1** (2), 19 (2010).
25. Thai, H. M. *et al.* Implantation of a three-dimensional fibroblast matrix improves left ventricular function and blood flow after acute myocardial infarction. *Cell Transplant*. **18** (3), 283-295 (2009).
26. Moreira Teixeira, L. S. *et al.* High throughput generated micro-aggregates of chondrocytes stimulate cartilage formation in vitro and in vivo. *Eur Cell Mater*. **23** 387-399 (2012).

27. Ifkovits, J. L. *et al.* Injectable hydrogel properties influence infarct expansion and extent of postinfarction left ventricular remodeling in an ovine model. *Proc Natl Acad Sci U S A.* **107** (25), 11507-11512 (2010).
28. Murphy, A. R., Laslett, A., O'Brien, C. M., & Cameron, N. R. Scaffolds for 3D in vitro culture of neural lineage cells. *Acta Biomater.* (2017).
29. Cheng, V. *et al.* High-content analysis of tumour cell invasion in three-dimensional spheroid assays. *Oncoscience.* **2** (6), 596-606 (2015).
30. Huber, J. M. *et al.* Evaluation of assays for drug efficacy in a three-dimensional model of the lung. *J Cancer Res Clin Oncol.* **142** (9), 1955-1966 (2016).
31. Lamichhane, S. P. *et al.* Recapitulating epithelial tumor microenvironment in vitro using three dimensional tri-culture of human epithelial, endothelial, and mesenchymal cells. *BMC Cancer.* **16** 581 (2016).
32. Ware, M. J. *et al.* Generation of an in vitro 3D PDAC stroma rich spheroid model. *Biomaterials.* **108** 129-142 (2016).
33. Monjaret, F. *et al.* Fully Automated One-Step Production of Functional 3D Tumor Spheroids for High-Content Screening. *J Lab Autom.* **21** (2), 268-280 (2016).
34. Shologu, N. *et al.* Recreating complex pathophysiologies in vitro with extracellular matrix surrogates for anticancer therapeutics screening. *Drug Discov Today.* **21** (9), 1521-1531 (2016).
35. Ho, W. J. *et al.* Incorporation of multicellular spheroids into 3-D polymeric scaffolds provides an improved tumor model for screening anticancer drugs. *Cancer Sci.* **101** (12), 2637-2643 (2010).
36. Pathak, A., & Kumar, S. Independent regulation of tumor cell migration by matrix stiffness and confinement. *Proc Natl Acad Sci U S A.* **109** (26), 10334-10339 (2012).
37. Wei, S. C. *et al.* Matrix stiffness drives epithelial-mesenchymal transition and tumour metastasis through a TWIST1-G3BP2 mechanotransduction pathway. *Nat Cell Biol.* **17** (5), 678-688 (2015).
38. Romero-Lopez, M. *et al.* Recapitulating the human tumor microenvironment: Colon tumor-derived extracellular matrix promotes angiogenesis and tumor cell growth. *Biomaterials.* **116** 118-129 (2017).
39. Xu, X., Sabanayagam, C. R., Harrington, D. A., Farach-Carson, M. C., & Jia, X. A hydrogel-based tumor model for the evaluation of nanoparticle-based cancer therapeutics. *Biomaterials.* **35** (10), 3319-3330 (2014).
40. Xu, X. *et al.* Recreating the tumor microenvironment in a bilayer, hyaluronic acid hydrogel construct for the growth of prostate cancer spheroids. *Biomaterials.* **33** (35), 9049-9060 (2012).
41. Nyga, A., Loizidou, M., Emberton, M., & Cheema, U. A novel tissue engineered three-dimensional in vitro colorectal cancer model. *Acta Biomater.* **9** (8), 7917-7926 (2013).
42. Yip, D., & Cho, C. H. A multicellular 3D heterospheroid model of liver tumor and stromal cells in collagen gel for anti-cancer drug testing. *Biochem Biophys Res Commun.* **433** (3), 327-332 (2013).
43. Hoare, T. R., & Kohane, D. S. Hydrogels in drug delivery: Progress and challenges. *Polymer.* **49** (8), 1993-2007 (2008).
44. Delgado, L. M., Bayon, Y., Pandit, A., & Zeugolis, D. I. To cross-link or not to cross-link? Cross-linking associated foreign body response of collagen-based devices. *Tissue Eng Part B Rev.* **21** (3), 298-313 (2015).
45. Florczyk, S. J. *et al.* Porous chitosan-hyaluronic acid scaffolds as a mimic of glioblastoma microenvironment ECM. *Biomaterials.* **34** (38), 10143-10150 (2013).
46. Kimlin, L. C., Casagrande, G., & Virador, V. M. In vitro three-dimensional (3D) models in cancer research: an update. *Mol Carcinog.* **52** (3), 167-182 (2013).
47. Zhang, M., Boughton, P., Rose, B., Lee, C. S., & Hong, A. M. The use of porous scaffold as a tumor model. *Int J Biomater.* **2013** 396056 (2013).
48. Wang, J. *et al.* Engineering EMT using 3D micro-scaffold to promote hepatic functions for drug hepatotoxicity evaluation. *Biomaterials.* **91** 11-22 (2016).